Proceedings of the 2022 International Conference on Smart Manufacturing and Material Processing (SMMP2022), A. Nayyar (Ed.)

doi:10.3233/ATDE220831

Numerical Thermal Analysis of Cold Plate Embedded in Novel Multistage Tesla Valve

Jun DU [a, 1], Yong LIU [a], Fan REN [a], Jing GUO [a], Menghan LI [a] and Samaneh ARMAN [b]
[a] *School of Energy and Power, Jiangsu University of Science and Technology, Zhenjiang, Jiangsu, China*
[b] *School of Science and Technology, The University of Georgia, Tbilisi 0171, Georgia*

Abstract. Excessively high temperatures will interfere with the operation of the components and damage equipment. The key to fixing this is to generate uniform heat dissipation and maximize heat dissipation. This paper proposed a cold plate with three S-type multistage Tesla valves (ST-MSTV). Thermal performance was first evaluated with flow direction and angle. The effects of channel flow direction and valve spacing on the cold plate were then investigated with Ansys Fluent software. The standard deviation of temperature was helpful in representing the uniformity of the temperature of the cold plate. The heat transfer capability of the three-channel ST-MSTV was proven to be effective on the fact that reverse flow causes fluid mixing and vortices. The flow channel form of scheme 2 is better than other schemes, showing the best temperature uniformity and the most effective cooling performance when the valve spacing is 30 mm.

Keywords. S-type multi-stage Tesla valve, Valve spacing, Temperature standard deviation, Temperature uniformity, Three-channel cold plate.

1. Introduction

The cold plate, an indirect liquid cooling technique, is popular in data centers, the aerospace industry, and automobile batteries because of its high heat transfer efficiency. The two-phase cold plate liquid cooling system is more complicated than a single-phase cold plate liquid cooling system because of the evaporative vaporization of liquid in the small liquid channel, which can affect the stability of coolant flow and eventually cause overheating.by causing pressure and temperature fluctuations. We explore the Tesla valve structure with a distinctive form to improve the cold plate's heat exchange effect. The Tesla valve structure is a one-way check valve without any internal moving elements that Nikola Tesla first proposed in 1920 and was first intended to control gas flow [1]. Early studies on Tesla valve structure were primarily focused on fluid characteristics [2-6].

And individuals have started to turn toward heat exchange in recent years as networks have grown and new technologies have emerged. To improve the heat transfer efficiency of a flat plate oscillating heat pipe (FP-OHP), Thompson et al. combined capillary/micrometer Tesla valves [7]. By stringing together valves in series, Porwal et

[1] Corresponding Author: Jun Du, e-mail: 961507537@qq.com

al. created multi-stage Tesla valves (MSTV) [8]. They then performed a three-dimensional numerical analysis of individual valves with MSTVs (up to 10 stages), and they derived and provided power law correlations for MSTV design and performance in terms of Nusselt number, Darcy friction factor, pressure duality, and thermal duality.

Based on the Tesla valve structure, Monika et al. combined the cold plate with the Tesla valve structure to propose a liquid cooling plate in the Tesla valve configuration for electric vehicle tram cooling [9]. A multistage Tesla valve with forward and reverse flow configurations was designed and analyzed to improve the inherent temperature gradient problem in conventional rectangular channels under turbulent flow conditions. The COMSOL Multiphysics software was used to study the effects of four parameters: the number of channels, the distance between two consecutive valves, the coolant temperature and heat flux applied to the top and bottom surfaces of the cooling plate at different Re numbers, and the cooling plate with four channels and a valve-to-valve distance of 8.82 mm showed the most efficient heat transfer capacity.

In this paper, an S-type multi-stage Tesla valve structure (ST-MSTV) is designed based on the study of Monika et al [9]. The current study is to design a single-stage Tesla valve and a 3D numerical model of the ST-MSTV embedded cold plate using Ansys Fluent software. First, transient and steady-state studies of the single-stage Tesla valve were performed to verify the relationship between heat exchange and flow direction. Second, a multiangle analysis of the angles involved in the Tesla valve was performed to find the optimal heat exchange angle. Subsequently, the flow direction and lateral spacing of the three-channel ST-MSTV cold plate were studied and analyzed as variables.

2. Methods

2.1. Model Setting

The Tesla valve is unidirectional and is divided into forward and reverse flow in different flow directions. After being improved by many generations, the GMF valve designed by Gambol et al. is considered to be the best as of now [10], based on which we adopt the MSTV designed by Thompson et al. and improve it to design the S-type multi-stage Tesla valve (ST-MSTV) [11]. The ST-MSTV in this study uses three channels with the number of stages N = 10, as shown in figure 1(a). The single-stage GMF valve consists of a straight section, a mixing section, an inclined section, a circular section (corresponding to the dimensions in figure 1(b): L1=120mm, L2=60mm, L3=180mm), and a diversion angle A and a convergence angle B.

The dimensions of the cold plate designed in this paper are 930.4 mm × 671.6 mm × 10 mm, and the rest of the parameters are shown in Table 1. To reduce the complexity of the structure and increase the display of the heat transfer effect of the structure, we choose the entire cold plate's upper and lower surfaces using uniform constant heat flow and ignore the thickness of the upper and lower surfaces of the valve structure. At the same time, to calculate the convenience and simplification, we assume that (1) the cold plate material is uniform and isotropic, (2) the coolant behaves as a single phase, (3) Newtonian fluid, (4) incompressible, (5) thermophysical properties and temperature independent, (6) steady state, (7) flow perpendicular to gravity, etc.

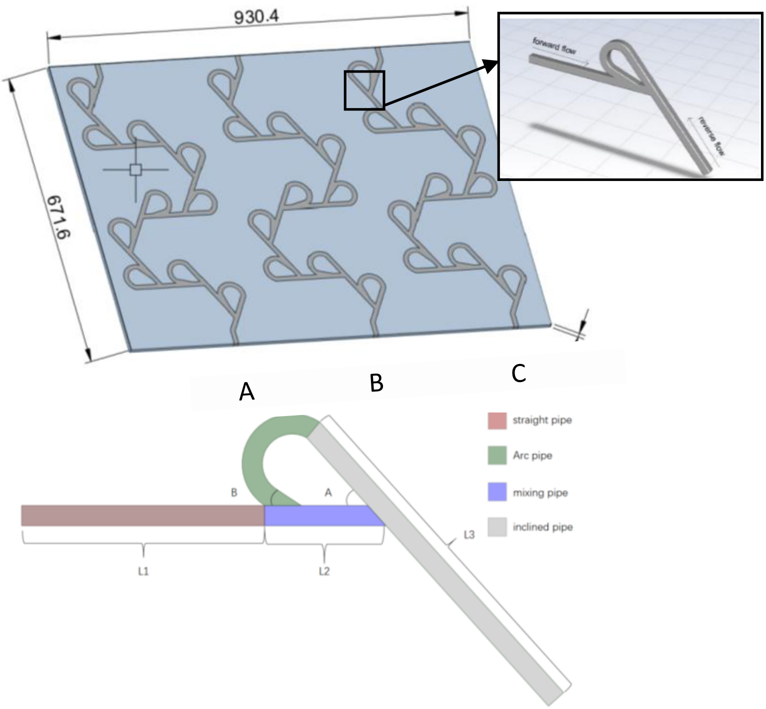

(b)

Figure 1. (a) Schematic diagram of the ST-MSTV 3D cold plate.

(b) dimensional drawing of the single-stage GMF-type Tesla valve.

2.2. Boundary Conditions

- Inlet: Velocity inlet, the flow rate of the controlled fluid is simulated numerically from 1000 to 10000 for Re, which is defined as:

$$\mathrm{Re} = \frac{\rho v \mathrm{d}}{\eta} \tag{1}$$

where ρ is the fluid density, v is the fluid flow rate, d is the characteristic pipe size, d = 10 mm for the Tesla valve understudy, and η is the dynamic viscosity coefficient.

- Outlet: Pressure outlet, 0 pressure.
- Wall: Stationary wall, no slippage.
- Interface: Coupling.
- Heat: A constant heat flow of 4000W/m2 is applied to the upper and lower surfaces of the plate, while the surrounding of the cold plate is assumed to be adiabatic conditions.

2.3. The Standard Deviation of Temperature.

In the center of the cold plate (5mm), according to the distribution of the extreme values of the hot spots, 14 measurement points are selected (Figure 2). To indicate the heat transfer uniformity of the cold plate, we use the temperature standard deviation as an evaluation index to analyze; the temperature standard deviation is defined as:

$$\sigma_T = \sqrt{\frac{\sum_{i=1}^{n}(T_i - \overline{T})^2}{n}} \tag{2}$$

where n is the number of measurement points; T_i is the temperature of the measurement point; $\overline{T}$ is the average temperature of the measurement point:

$$\overline{T} = \frac{\sum_{i=1}^{n} T_i}{n} \tag{3}$$

Therefore, the smaller σ_T indicates the more uniform heat transfer. Also, the performance of the cold plate is expressed as T_{max}, which can reflect the worst case of heat exchange of the cold plate by ST-MSTV.

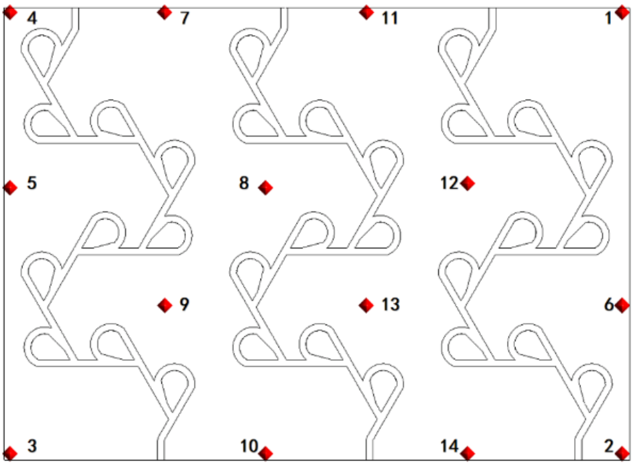

Figure 2. Schematic diagram of the location of the measurement points (No. 1).

3. Results and Discussion

3.1. Heat Transfer Characteristics

Figure 3(a) (b) shows the heat transfer contour plots for a GMF-type valve structure with fluid flowing in both forward and reverse directions at Re=1000 and a fluid temperature of 293K. Figure 3(c) (d) shows the heat transfer contour plot for a given initial wall temperature (T=343K) for the same number of Re at a transient state. From the plot, we can see that the pipe temperature rises more for the fluid in the reverse flow compared to the forward direction, which indicates that the wall produces a stronger heat transfer effect with the fluid in the reverse flow. This is due to the reverse flow, fluid flow along the straight channel, when encountered along the flow direction of the acute branch and will be due to fluid flow oscillation generated by the diversion, part of the fluid will flow to the acute branch, of course, the mainstream of fluid or most continue to flow along the straight channel flow to the arc pipe and change the direction of flow. Fluid convergence leads to fluid flow mixing and vortex to strengthen the strong fluid heat transfer. From the figure, we also observe that the temperature of the inner side of the arc pipe is higher than the outer side, which is due to a certain speed of fluid flow into the arc pipe due to the role of centrifugal force leading to fluid bias to the outer side of the arc pipe flow.

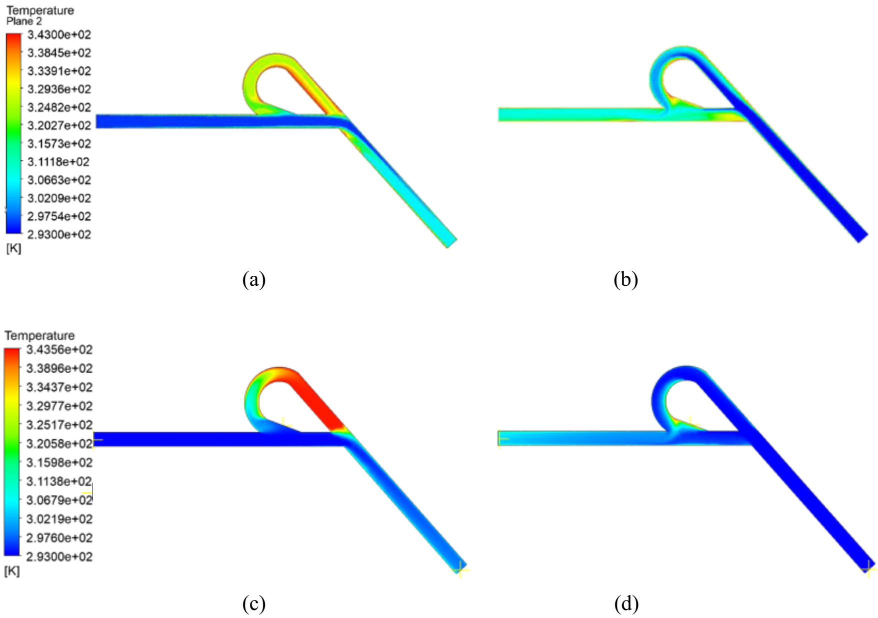

Figure 3. GMF type Tesla valve structure, Re=1000, T=343K: steady state: (a) forward (b) reverse; transient: t=3s: (c) forward (d) reverse.

3.2. Effect of Different Angles on Heat Transfer

Through the above study, we know that for the Tesla valve structure, the heat transfer effect of reverse flow is better than that of forward flow, and different split fluid angles and confluence angles may affect the heat transfer strength in reverse flow. For this reason, we conducted five split fluid angles and six confluence angles for a single Tesla valve structure, respectively, and used the control variable method to control the fluid temperature, inlet flow rate, tube wall temperature, and other conditions to keep the same, and adopted the inlet and outlet temperature difference as the evaluation index to analyze the heat transfer effect, and the results obtained are shown in Figure 4. A comparison of six convergence angles at 40 ° and 48 ° split fluid angles was carried out, and from the figure we can see that among the six confluence angles in the sample, the 15 ° confluence angle has the largest inlet and outlet temperature differences of 21.2 K and 22 K, respectively. This is consistent with what is expected because the larger the confluence angle, the greater the hedging strength of mainstream and diversion, thus making the hedge generated by the mixing, the vortex more intense, increasing the heat transfer coefficient.

For the split fluid angle, based on the confluence angle of 15 ° , we investigate five split fluid angles, and the results are shown in figure 4 (b). We found that as the angle of split fluid increases, the temperature difference between the input and outlet increases. This is because the increased angle of the split fluid leads to a longer distance for the circular pipe to converge with the branch, thus increasing the heat transfer area. Of course, too large a split fluid angle tends to lead to a less and less fluid split and gradually close to the result of forward flow.

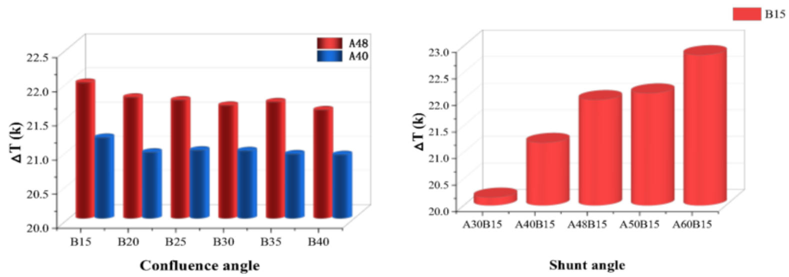

(a) (b)

Figure 4. The temperature difference between inlet and outlet of the Tesla valve structure at different angles (a) confluence angle (b) split fluid angle

3.3. Effect of Different Flow Directions on ST-MSTV

In this study, the effect of flow direction was discussed for a three-channel S type multistage Tesla valve (N=-10), and the flow direction groupings are shown in Table 1. due to the symmetry of the cold plate, some of the combinations overlap, so eight combinations were selected to obtain four final study groups, numbered 1, 2, 3, and 8. (Up and down are the inlet flow directions).

Table 1. Combinations of different flow directions of 3 channel S-type MSTV

Combination number	Channel A	Channel B	Channel C
1	up	up	up
2	up	up	down
3	up	down	up
4	up	down	down
5	down	down	down
6	down	down	up
7	down	up	down
8	down	up	up

In the above four scenarios, we conducted comparative studies with Re=1000, the fluid temperature of Tin=283K, and keeping the wall heat flow density q=4000w/m2, respectively. Fourteen measurement points were selected in the center of the cold plate at 5 mm according to the hot spot extreme value distribution (Figure 2) and kept the location of the measurement points constant, and the results were obtained as shown in Figure 5, all the measurement points were in the center of the cold plate thickness. Since the average temperature of the measurement points of the four schemes is within 359K (±1K) (shown in Table 2), 359K is set as the average temperature value, and the temperature of all the measurement points of the four schemes is scattered in the figure. From the figure we can find that measurement point 5 to measurement point 14 is more uniform that the magnitude of the average temperature gap is smaller, while measurement point 1 to measurement point 4 shows a larger magnitude, mainly because the four measurement points are located in the four right-angle positions of the cold plate, each only by a channel on its heat exchange, heat exchange compared to other measurement points less (figure 6).

From Table 2 we can obtain that, compared to the other schemes, Scheme 2 has a lower temperature maximum (T_{max}) = 379 K and a lower temperature standard deviation (σ_T =13.87), which indicates that Scheme 2 has good homogeneity.

Table 2. Measurement point data.

Number	T_{ave}	T_{max}	σ_T
1	358.6637143	407	19.95554269
2	359.5789286	379	13.87166566
3	359.3505	409	19.90527063
8	358.1569286	407	23.77202654

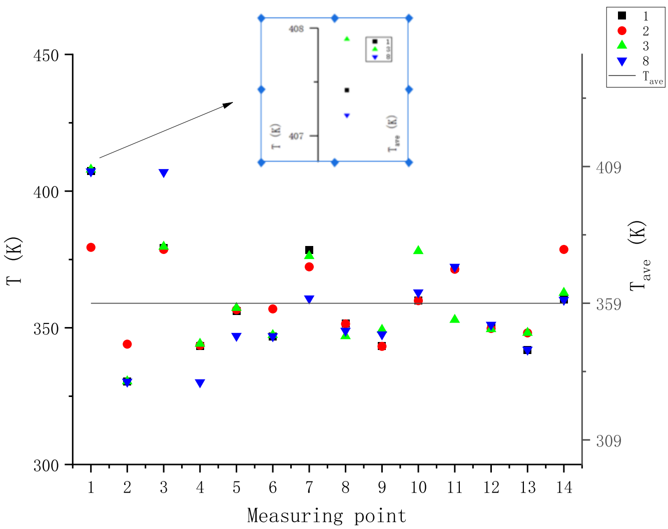

Figure 5. Temperature scatter plot of measurement points for 4 combinations.

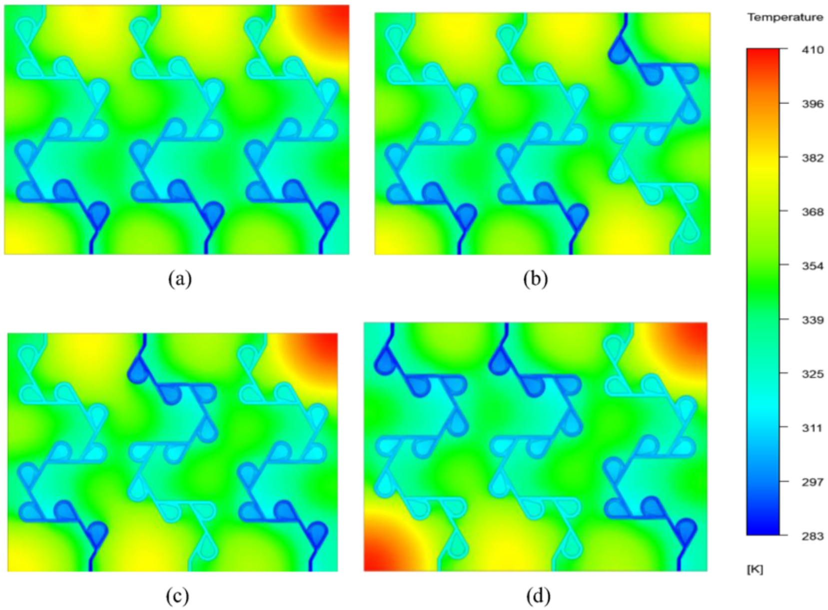

Figure 6. Temperature distribution of the four flow channels of No. 2 (a) No. 1 (b) No. 2 (c) No. 3 (d) No. 8.

3.4. Effect of Different Horizontal Spacing on ST-MSTV

In scheme numbered 2, the lateral spacing of the 10-stage ST-MSTV was adjusted for five sizes: 10, 20, 30, 40, and 50 mm. Figure 7 (a) shows the maximum value of the cold plate temperature, the average value of the temperature, and the standard deviation of the measured point temperature for the different spacing of the ST-MSTV.

From the figure we can see that the average temperature of the cold plate gradually decreasing as the transverse pitch increases, the pitch increases from 10 mm to 50 mm, and T_{ave} decreases by 5.7 K. This indicates that increasing the pitch has a positive effect on the heat transfer of the cold plate to some extent, which is due to increasing the pitch while increasing the heat transfer area. Different from the results of T_{max} and σ, which we can see in Figure 7 (a), they have a very different trend from T_{ave}. The increase in spacing does not lead to a constant decrease in T_{max}, but produces a very small value at 30 mm spacing, while the standard deviation of the measured point temperature also reaches a very small value of 13.8 at 30 mm, which indicates that the spacing cannot be increased to optimize the heat transfer effect.

The above results are due to the fixed distances between channels 1 and 3 from the cold plate boundary. Increasing the spacing, on the one hand, is to reduce the heat transfer distance between the channels, thereby reducing the need for heat transfer area, and on the other hand, the space between the two channels that needs to be covered with cold water becomes smaller. And the sacrifice is the cold plate edge of the heat transfer effect, cold water heat transfer to cover the distance becomes far from the edge of the cold plate, resulting in the temperature of that part is higher than the surrounding part. As shown in figure 7 (b-f), we can see the change between measurement point 1 and measurement point 14: as the distance increases, the temperature of measurement point 14 gradually decreases while the temperature of measurement point 1 gradually increases (Table 3).

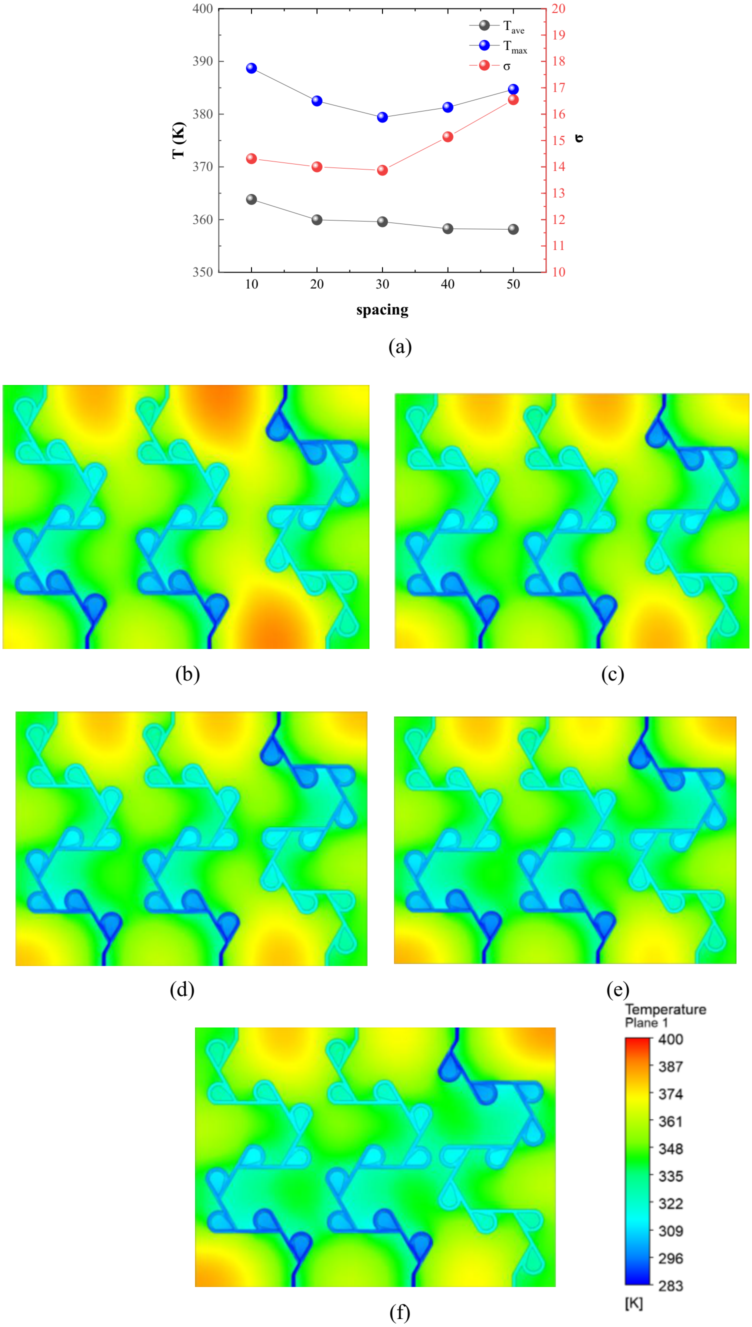

Figure 7. Re=1000, comparison at different spacings: (a) T_{max}, T_{ave}, and σ; temperature clouds (b) 10mm (c) 20mm (d) 30mm (e) 40mm (f) 50mm.

Table 3. Temperature comparison between measurement point 1 and measurement point 14.

Spacing(mm)	Measurement point14(K)	Measurement point1(K)
10	381.491	371.916
20	380.908	375.583
30	378.66	379.447
40	375.815	380.968
50	367.55	384.499

4. Conclusion

Compared to the forward flow, the reverse flow of fluid within the Tesla valve structure has a higher shunt rate, and the impact and mixing of the tributaries with the main flow lead to the creation of vortices, resulting in a higher heat transfer capacity for the reverse flow.

In the studied range of angles related to the valve structure, the shunt angle of 60 ° and the confluence angle of 20 ° have a higher heat transfer capacity for the reverse flow of fluid in the Tesla valve structure.

Changing the flow direction of the valve channels in the cold plate can affect the cooling effect of the cold plate, limited by the size of the cold plate in this study, so in the study range ST-MSTV is 10 levels and the number of channels is 3, limited to this structure, the best flow direction obtained is option 2, ie. channels 1 and 2 flow up and channels 3 flow down.

Different transverse valve spacing will cause the cold plate T_{max} to appear in different places, roughly divided into two areas, respectively, measurement point 1 and measurement point 14. increasing the spacing will cause the temperature at measurement point 1 to rise, and decreasing the spacing will cause the temperature at measurement point 14 to rise, so the optimal spacing is obtained as 30 mm.

References

[1] N. Tesla, “Valvular conduit,” U.S. Patent 1329559, Feb 03, 1920.

[2] R.L. Bardell, M. Microsciences, The diodicity mechanism of Tesla-type no-moving-parts valves, PhD thesis, University of Washington (2017).

[3] T. Wahidi, R.A. Chandavar, A.K. Yadav, Stability enhancement of supercritical CO2 based natural circulation loop using a modified Tesla valve, J. Supercrit. Fluids 166 (2020) 105020.

[4] Anagnostopoulos, J. S., and Mathioulakis, D. S., 2005, “Numerical Simulation and Hydrodynamic Design Optimization of a Tesla-Type Valve for Micro-pumps,” Proceedings of the Third IASME/WSEAS International Conference on Fluid Dynamics and Aerodynamics, Corfu, Greece, Aug. 20–22, pp. 195–201.

[5] Abdelwahed, M., Chor, N., and Malek, R., 2019, “Reconstruction of Tesla Micro-Valve Using Topological Sensitivity Analysis,” Adv. Nonlinear Anal., 9 (1), pp. 567–590.

[6] Ren Pu and Long Wei. Numerical analysis of Tesla valve flow field characteristics and cavitation formation mechanism. Journal of Southwestern University (Natural Science Edition), 2021, 43 (08): 161-166. DOI: 10.13718/j.cnki.xdzk.2021.08.020.

[7] S. M. Thompson, H. Ma, and C. Wilson, “Investigation of a flat-plate oscillating heat pipe with tesla-type check valves”, Exp. Therm. Fluid Sci., vol. 35, no. 7, pp. 1265–1273, 2011. DOI: 10.1016/j.expthermflusci.2011.04.014.

[8] P. R. Porwal, S. M. Thompson, D. K. Walters, T. Jamal, Heat transfer and fluid flow characteristics in multistaged Tesla valves, Numer. Heat Transf. Part A: Appl. 73(2018) 347–365. doi:10.1080/10407782.2018.1447199

[9] K. Monika, C. Chakraborty, S. Roy, R. Sujith, Santanu Prasad Datta. A numerical analysis on multi-stage Tesla valve based cold plate for cooling of pouch type Li-ion batteries. International Journal of Heat and Mass Transfer, Volume 177 (2021) 121560.

[10] A. R. Gamboa, C. J. Morris, and F. K. Forster, "Improvements in fixed-valve micropump performance through shape optimization of valves," J. Fluids Eng., vol. 127, no. 2, pp. 339–346, 2005. DOI: 10.1115/1.1891151.

[11] S.M. Thompson, T. Jamal, B.J. Paudel, D.K. Walters, Transitional and turbulent flow modeling in a Tesla valve, in: Proceedings of the International Mechanical Engineering Congress and Exposition, 7 B, 2013.